Progress In Electromagnetics Research M, Vol. 110, 235–247, 2022

A Millimeter Wave Elliptical Slot Circular Patch MIMO Antenna for Future 5G Mobile Communication Networks

Suman Sharma* **and Mukesh Arora**

Abstract—This paper proposes a 4-port MIMO (Multiple-Input Multiple-Output) antenna operating at 28 GHz in the millimeter wave band for future 5G communications. The first design in this work is a single-element circular shaped microstrip patch antenna with an elliptical slot and a defected ground structure which is intended for 28 GHz band. This antenna is compact with a size of 6 mm × 7 mm. A complete analysis of single patch element antenna is presented with the effect of slot and defected ground structure in Section 2. In Section 3, the second design, which is symmetric two-element MIMO slotted circular patch antennas, is analyzed with the dimension $L \times W$ as 7 mm × 6 mm. In Section 4, the final fabricated design is presented, which is a 4-port MIMO antenna operating at the resonance frequency of 28 GHz along with the improved isolation between the elements due to appropriate spacing. The proposed 4 port MIMO antenna is designed on a Rogers Duroid 5880 substrate having a relative dielectric permittivity of 2.2 and thickness of 0.8 mm. The overall dimension of this designed MIMO antenna is $20 \times 20 \times 0.8\,\text{mm}^3$. Simulated results for the S-parameters and radiation pattern are presented for all purposed designs using CST software. Measured results are also presented for the return loss using Rhode & Schwarz ZVA 40 vector network analyzer. Simulated and measured results show a good agreement. The simulation results demonstrate that the return loss at individual port is less than −10 dB in the frequency range of 26.867–28.975 GHz, and it provides a bandwidth of 2.1 GHz. The antenna has a high gain of 9.24 dB with unidirectional radiation pattern, and each element has a mutual coupling less than −20 dB.

1. INTRODUCTION

Due to its capacity to offer high data rates and low latency, 5G technology has received a great deal of attention in today's era. Research has focused significantly on millimeter-wave front ends because bandwidth is directly related to higher data rates [1].

5G standard has allotted several frequency bands, including 28 GHz band as the most important (O2 band) and 164–200 GHz as the unlicensed spectrum (H2O band) [2, 3]. Compared to sub-6 GHz that has a remarkable number of applications, the higher spectrum is having less applications. Mm-wave spectrum is very susceptible to the atmospheric attenuations as the wavelengths become so small that alterations in the signal strength can degrade the experience of 5G [4].

As of now, 4G technology has been implemented. Yet, the technological improvements in the modern era were not able to satisfy the demands of higher data rates and bandwidth [5]. There is a high probability that mobile data traffic generated by applications, such as video streaming, social networking, and cloud computing, will exceed the capabilities of today's 4G networks [8]. To meet this demand, research is underway into Fifth Generation (5G) technology, and it has taken a lot of effort by researchers for 5G to become a universal standard. This is an exceptionally challenging task considering the increase in bandwidth and data rates [6, 7]. To take care of this issue, the Multiple-Input Multiple-Output (MIMO) advancements along with a wide data transmission are essential to further development

Received 11 April 2022, Accepted 25 May 2022, Scheduled 10 June 2022
* Corresponding author: Suman Sharma (sumansharma@skit.ac.in).
The authors are with the Swami Keshvanand Institute of Technology Management & Gramothan, Jaipur, India.

of channel limit and range effectiveness by using multipath property with no requirement for expanding the information power [8, 9]. Moreover, the attributes of proper isolation between the elements and broadband ought to be moved by the MIMO framework to add a successful execution [10, 11]. The throughput of the MIMO antenna system is influenced by the higher mutual coupling between the MIMO antenna elements [12, 13].

So, the design and development of a MIMO antenna along with a proper isolation between the elements is a tremendous challenge. 5G technology generally focuses on the centimeter and millimeter wave spectrum (3–300 GHz), and it helps attaining a higher bandwidth which can yield a data rate up to more than 20 Gigabit-per-second (Gbps) [14, 15]. Furthermore, the lower portion of the spectrum has already been used for several applications such as Wi-Fi, WiMAX, Bluetooth, ISM, and mobile communication. Furthermore, the higher portion of the spectrum is still untapped which can be utilized for the 5G technology [16]. The feasibility, advantages, and challenges of future wireless communications over the E band frequencies have been investigated in [17]. A Directional Radio Propagation Path Loss Model for Millimeter-Wave Wireless Networks in the 28, 60, and 73 GHz Bands is proposed in [18]. Different antennas have been proposed and analyzed for 5G applications [19–22], and several MIMO antennas have been highlighted [23–31], covering a large range of frequencies of the 5G spectrum. There have been different proposals for MIMO configurations for lower spectrum regions, including those below 6 GHz, while above 20 GHz, MIMO setups have also been proposed. A four element antenna structure is presented in [23] which covers the mm-wave frequency band of 25.5–29.6 GHz for 5G communication system with a peak gain of 8.3 dB. In [24], a MIMO array antenna along with a bandwidth of 3.4 to 3.6 GHz is proposed for 5G applications.

A MIMO antenna array with dual frequency bands and dimensions of $150 * 75 * 7\,\text{mm}^3$ has been presented in [26]. It has a bandwidth of 3.4 to 3.6 GHz and 4.8 to 5.1 GHz at -6 dB. In [27], an array of MIMO antennas is presented with a SIW-fed slot antenna. The frequency bands 27.5–28.35 GHz and 24.25–27.5 GHz are covered by this antenna for 5G, and the gain varies from 8.2 to 9.6 dB. A MIMO antenna covering the frequency range between 26 and 29.5 GHz with a peak gain of 14 dB for 5G applications is proposed in [28]. A 5G metamaterial-based antenna for MIMO systems presented in [29] offers a maximum gain value of 7.4 dB. A $66.8 \times 40 \times 0.8\,\text{mm}^3$ broadband MIMO antenna which has an impedance bandwidth of 2.6 to 13 GHz has been developed [30]. A four element MIMO antenna system of size $158 \times 77.8\,\text{mm}^2$ which covers the 5G frequency band 27.5 to 40 GHz is proposed in [31]. Using an arbitrary portion of the visible space, a novel method is proposed to synthesize fields that maximize the power radiated in the presence of beam efficiency limitations and protection requirements [33].

In this paper, a four element MIMO antenna for 5G mm-wave applications is proposed. This proposed antenna has a high gain, good efficiency, and good isolation among all ports.

The sequenced research work is described as follows. The geometry of the proposed single element antenna and its simulation results like s parameter, radiation pattern, E plane and H plane plots, surface current, etc. are presented in Section 2. In Section 3, a two element MIMO antenna is proposed, and its simulation results are analyzed. In Section 4, a four element MIMO antenna is proposed, simulated, and analyzed. A complete design procedure is explained through the flowchart given below.

2. SINGLE ELEMENT ANTENNA DESIGN

2.1. Antenna Geometry and Simulation Results

Figure 1 shows the proposed single element antenna design. Figures 1(a) and 1(b) show the front view and back view of the design. A description of the proposed antenna design parameters can be found in Table 1. Microstrip feed line technique is used to feed the antenna for $50\,\Omega$ impedance matching. A circular patch antenna with an elliptical slot and a defected ground structure is designed and simulated on a Rogers Duroid 5880 substrate having a relative dielectric permittivity of 2.2 and thickness of 0.8 mm. Initially, a single element circular patch antenna shown in Figure 2, without a slot and a defected ground structure, was designed and simulated using the same dimensions of patch, substrate, and ground. Then effects of cutting a slot and a DGS structure were analyzed. Figure 3 shows the simulated results of both of the designs which are shown in Figure 1 and Figure 2.

To obtain a frequency shift to the desired frequency of operation, an elliptical slot was cut at top surface of the circle, then S_{11} parameter was realized, which is shown in Figure 4(a). Further, to get

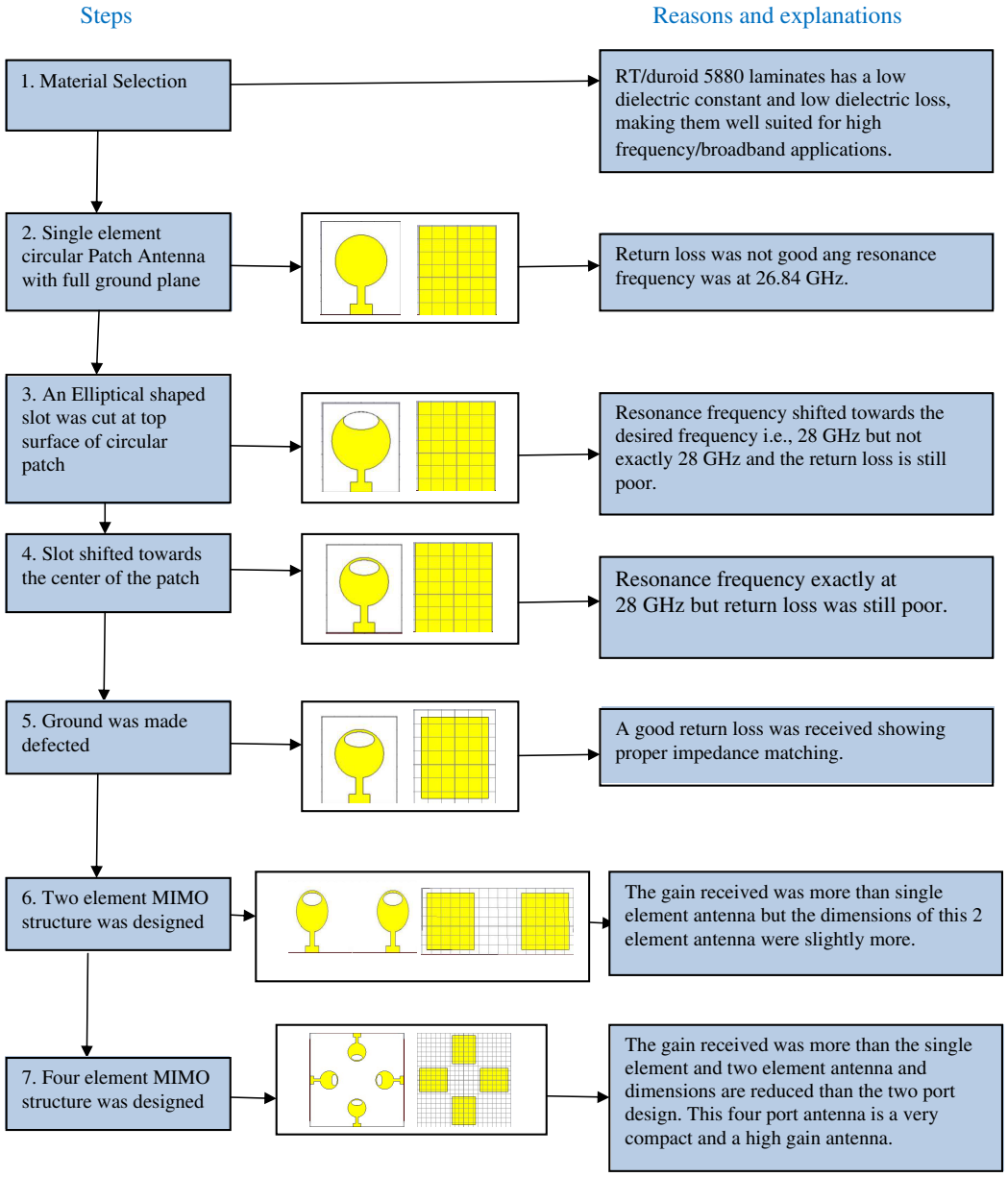

Flow Chart of Complete Design Procedure

Table 1. Dimensions of single element antenna.

Parameter	Value (mm)	Parameter	Value
Substrate width W_s	6	Patch Diameter D	3.94
Substrate length L_s	7	Elliptical slot x diameter D_x	2.4
Feed width W_f	1.68	Elliptical slot y diameter D_y	1.2
Feed Length L_f	1.32	Ground Width W_g	5
		Ground Length L_g	6

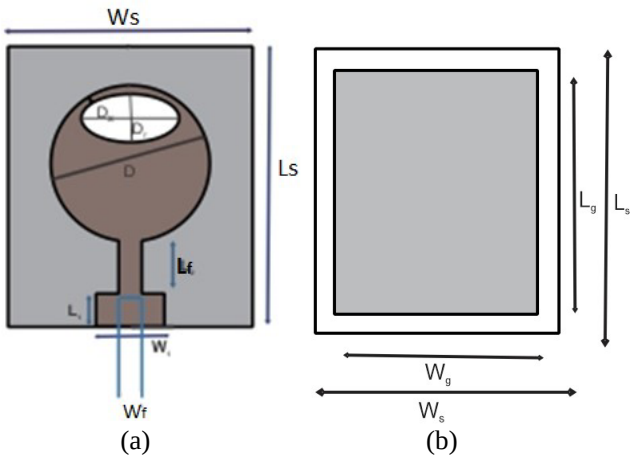

Figure 1. The proposed antenna design. (a) Front view, (b) back view.

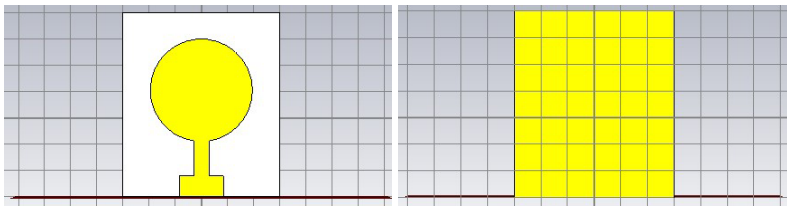

Figure 2. Antenna design without slot and without DGS. (a) Front view, (b) back view.

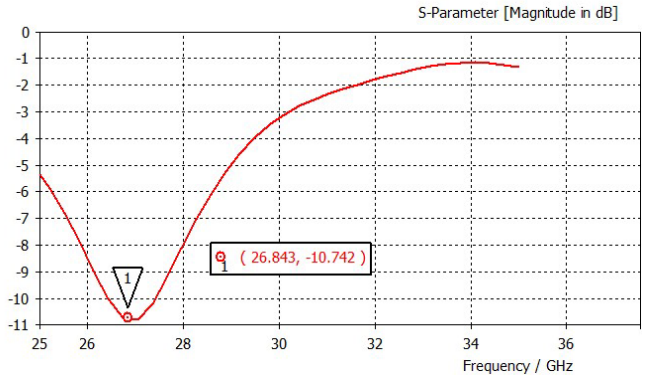

Figure 3. Return loss without slot and without DGS.

a better impedance matching and resonance frequency exactly at 28 GHz, the slot was shifted towards the center. Simulation result of return loss of slot shifting is shown in Figure 4(a), and the effect of partial ground plane is shown in Figure 4(b).

2.2. Radiation Pattern, Surface Current Distribution and Polar Plot

Figure 5 shows the radiation pattern of unit element antenna which is unidirectional, and the gain obtained is 6.1 dB. Surface current distribution in Figure 6 shows that most of the current flow is concentrated around the surface of the patch and on the feed line. Figure 7 shows the E field and H field plots of single element antenna. The direction of main lobe is 0 degrees.

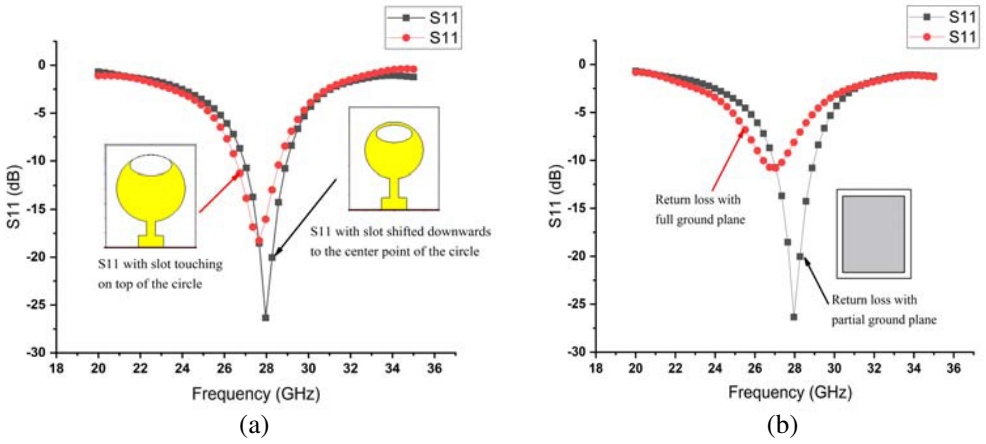

Figure 4. Simulated return loss. (a) Effect of slot shifting, (b) effect of partial ground plane.

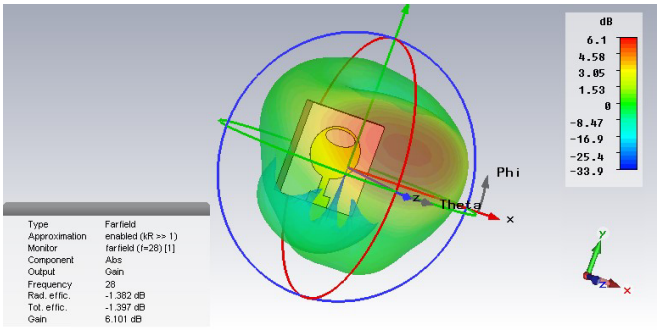

Figure 5. 3D radiation pattern of single element antenna design.

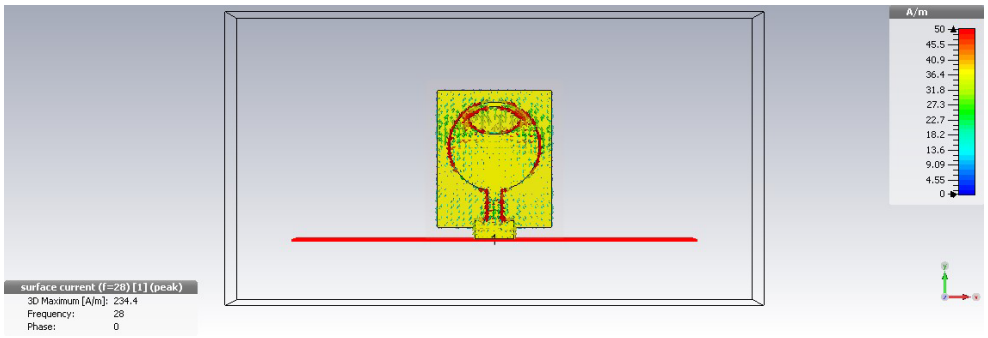

Figure 6. Surface current distribution of single element antenna.

3. TWO ELEMENT MIMO ANTENNA

The two element MIMO antenna with same dimension of patch, slot, and ground is presented in Figure 8. Figures 8(a), (b) show the front view and back view of the two port patch antenna with substrate dimension as 16 mm × 7 mm. Figure 8(c) shows that the return loss at 28 GHz is −30.07 dB, and there is a good isolation between the two antenna elements. 3D radiation pattern is shown in Figure 8(d) with the increased gain of 7.57 dB.

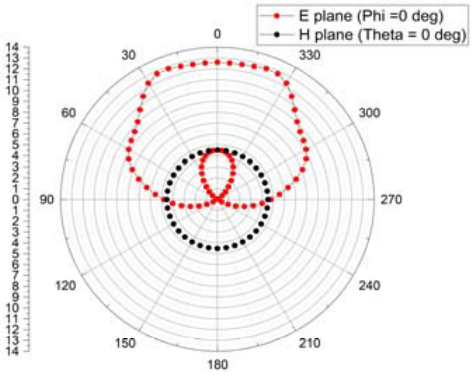

Figure 7. E plane and H plane plot of purposed single element antenna.

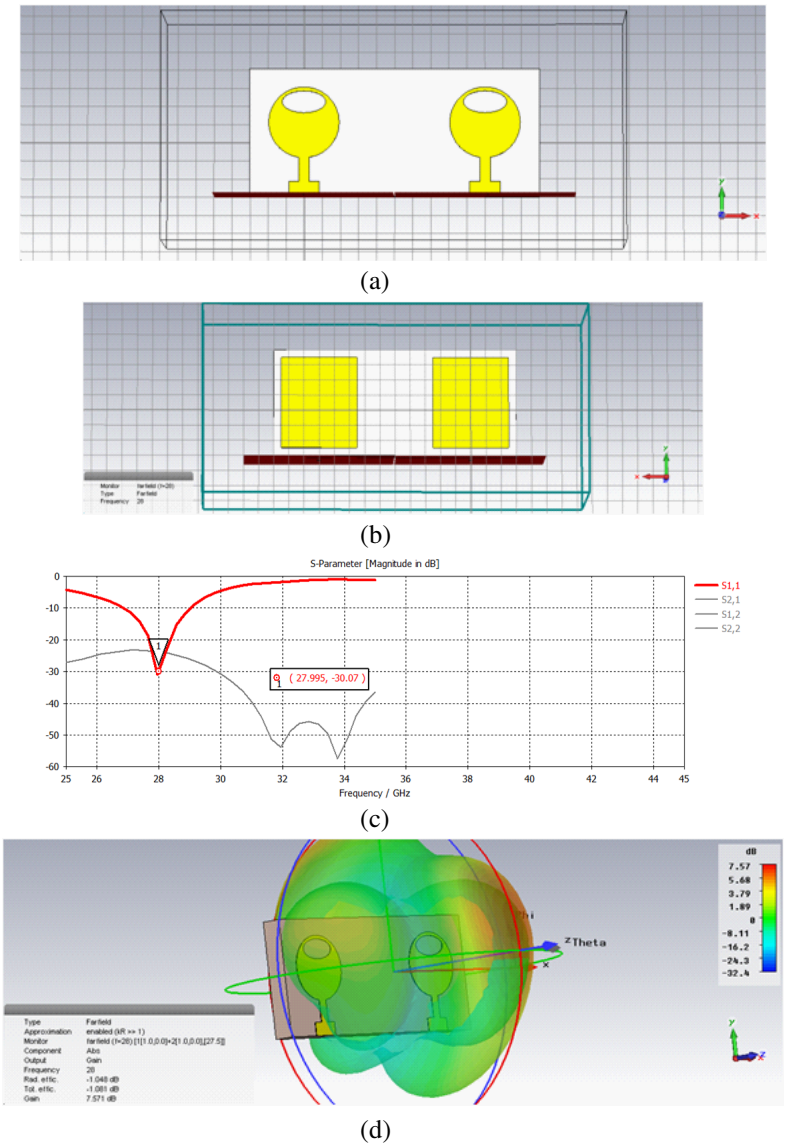

Figure 8. Two element MIMO antenna structure and its simulation results.

4. FOUR ELEMENTS MIMO ANTENNA CONFIGURATION

A four element MIMO antenna is proposed as shown in Figure 9, by using the single antenna element design that was proposed in Section 2. The overall dimension of this antenna is $20 \times 20\,\text{mm}^2$, with each of the four elements placed symmetrically and in rotational of 90-degree interval to form a square. The proposed MIMO antenna achieves greater than 18 dB isolation among all the four ports.

In MIMO systems, the presence of many similar elements results in higher mutual interference and an increase in Envelope Correlation Coefficient (ECC) among the different antenna elements. So, it is a difficult task to design a four port diversity antenna due to the mutual interference between the radiating elements. Because of this, the diagonal elements in the four element MIMO antenna are arranged in an anti-parallel manner, while the four elements are arranged orthogonally with each other. The fabricated 4 port MIMO antenna for 5G is shown in Figure 10. Figure 11 shows the surface current

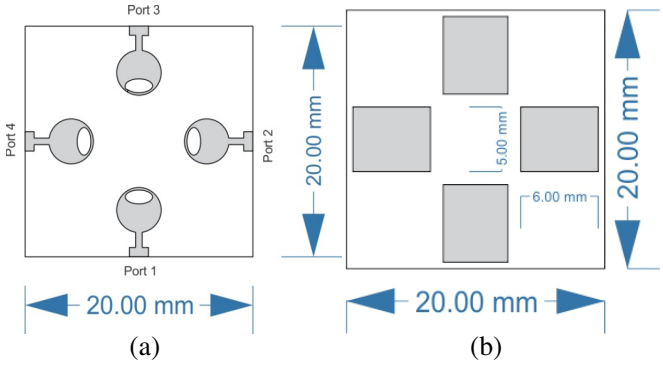

Figure 9. Purposed four element MIMO antenna structure.

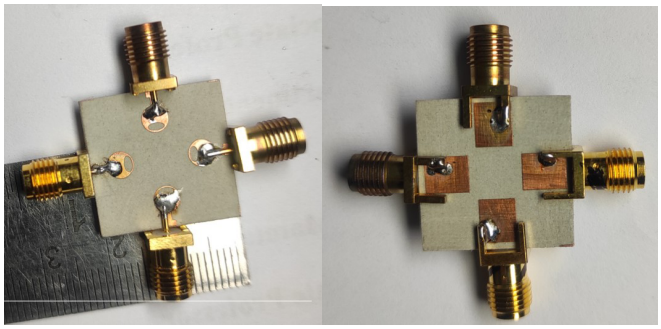

Figure 10. Fabricated four port MIMO antenna design.

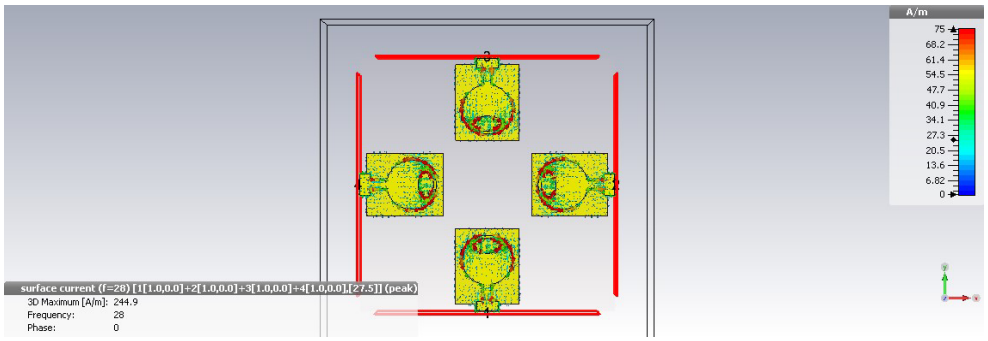

Figure 11. Surface current distribution of a four-port MIMO antenna.

distribution of a four-port MIMO antenna on simultaneous excitation of all four ports at a frequency of 28 GHz. A maximum flow of current has been observed around the feed line of the proposed MIMO antenna elements and along the edges of the circles. The coupling current is relatively insignificantly concentrated between elements of MIMO antennas.

4.1. Definitions and Equations of Reflection Coefficients and Transmission Coefficients of All Four Ports

The ratio of the amplitude of the reflected wave to that of the incident wave is termed as Reflection Coefficient. Similarly, the ratio of the amplitude of the transmitted wave to that of the incident wave is called Transmission Coefficient. A four port antenna network is shown in Figure 12, where

a_1 = Incident Normalized wave at port 1, b_1 = Reflected normalized wave at port 1
a_2 = Incident Normalized wave at port 2, b_2 = Reflected normalized wave at port 2
a_3 = Incident Normalized wave at port 3, b_3 = Reflected normalized wave at port 3
a_4 = Incident Normalized wave at port 4, b_4 = Reflected normalized wave at port 4

$$S_{ij} = \frac{\textit{Normalized transmitted/reflected wave voltage at ith port}}{\textit{Normalized incident wave voltage at ith port}}$$

$$S_{11} = \frac{b_1}{a_1}, \quad S_{12} = \frac{b_1}{a_2}, \quad S_{13} = \frac{b_1}{a_3}, \quad S_{14} = \frac{b_1}{a_4}$$

So, the total reflected wave at port 1 =

$$b_1 = S_{11}a_1 + S_{12}a_2 + S_{13}a_3 + S_{14}a_4 \tag{1}$$

In the same way,

$$b_2 = S_{21}a_1 + S_{22}a_2 + S_{23}a_3 + S_{24}a_4 \tag{2}$$
$$b_3 = S_{31}a_1 + S_{32}a_2 + S_{33}a_3 + S_{34}a_4 \tag{3}$$
$$b_4 = S_{41}a_1 + S_{42}a_2 + S_{43}a_3 + S_{44}a_4 \tag{4}$$

From Equations (1), (2), (3) and (4) —

$$\begin{bmatrix} b_1 \\ b_2 \\ b_3 \\ b_4 \end{bmatrix} = \begin{bmatrix} S_{11} & S_{12} & S_{13} & S_{14} \\ S_{21} & S_{22} & S_{23} & S_{24} \\ S_{31} & S_{32} & S_{33} & S_{34} \\ S_{41} & S_{42} & S_{43} & S_{44} \end{bmatrix} \begin{bmatrix} a_1 \\ a_2 \\ a_3 \\ a_4 \end{bmatrix}$$

Transmission Coefficients — Reflection Coefficients

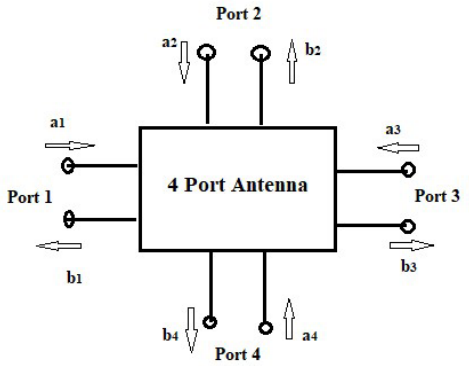

Figure 12. Four port antenna network.

4.2. Simulated and Measured Results

In this section, the simulated and measured results are analyzed in detail. Four SMA end launch jack 1.57 mm PCB 0–40 GHz connectors are used to feed the elements of the MIMO antenna. The simulation was carried out on CST Studio Suite while the antenna measurements are carried out on Rhode & Schwarz ZVA 40 vector network analyzer. The measurement of transmission and reflection coefficients is performed by terminating idle ports in 50 Ω load on the fabricated quad-element MIMO antenna.

4.3. *S* Parameters

The simulated and measured results of reflection coefficients and transmission coefficients of all four ports are shown in Figures 13(a) and 13(b), respectively. There is a good agreement between the results. Simulated results show that $S_{11} = S_{22} = S_{33} = S_{44} = -30$ dB on resonance frequency 28 GHz while the measured S parameters for all four ports are −25 dB on the same resonance frequency. The proposed MIMO antenna has a 2.1 GHz bandwidth based on the −10 dB criterion. MIMO antenna elements show a mutual interference of less than −20 dB over the entire region of interest as shown in Figure 13(b). It can be observed that there is a slight variation in simulated and measured results due to the cable losses. A photograph at the time of measurement of S parameters on Rhode & Schwarz ZVA 40 VNA is included in Figure 14.

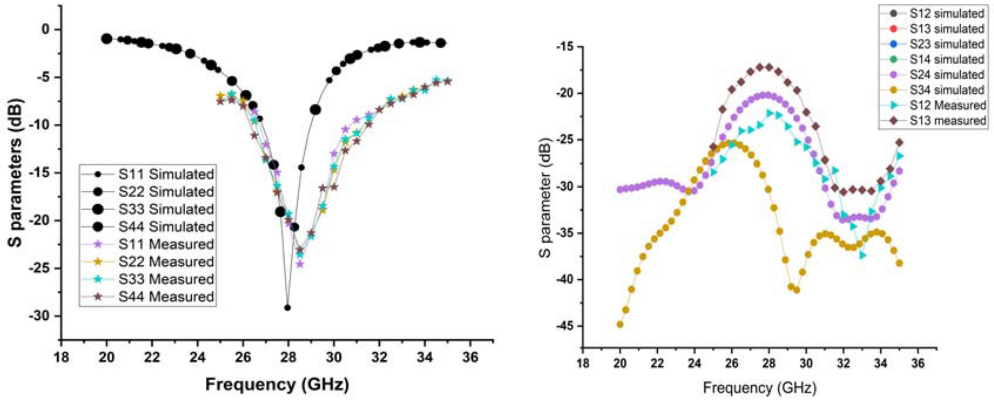

(a) (b)

Figure 13. Simulated and measured results of (a) reflection coefficients and (b) transmission coefficients of all four ports.

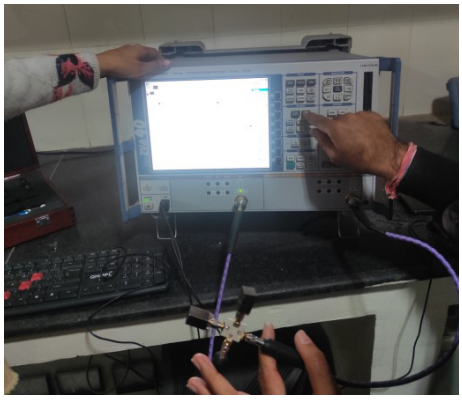

Figure 14. Photograph of measurement of S parameters on Rhode & Schwarz ZVA 40 VNA.

4.4. Far Field Measurement

Figure 15 shows the radiation pattern of the four elements MIMO antenna. It can be noted from the figure that the 3D gain of the MIMO antenna is 7.69 dB on 28 GHz frequency, and the MIMO antenna system produces a directional radiation pattern. In Figures 16(a) and (b), the radiation patterns for two principal planes, i.e., E-plane and H-plane, at 28 GHz are shown.

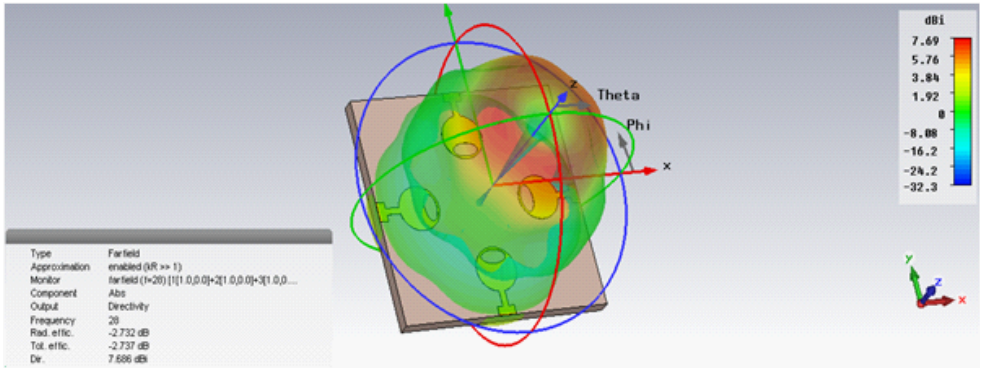

Figure 15. Radiation pattern of purposed four elements MIMO antenna.

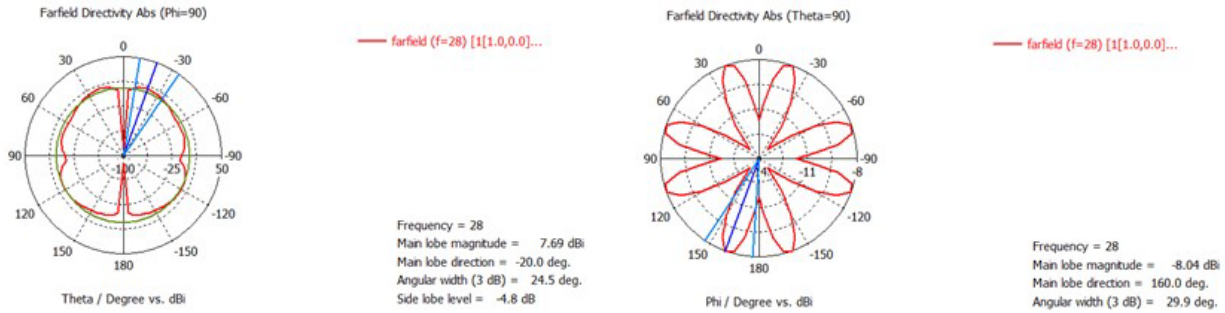

Figure 16. E filed and H field plot of 4 element MIMO antenna.

The beam efficiency of an antenna may be defined as the ratio of the power radiated within the main beam to the total power radiated. In the proposed 4 port MIMO antenna, the beam efficiency is improved as we can see that side lobe level power is −5 dB which is very low, so most of the power is concentrated in the main lobe at a fixed direction that is around 20 degrees shifted from the main orthogonal direction of the antenna. This will help to serve mobiles and other wireless devices to have a directive pattern.

As shown in Figure 17, the proposed MIMO antenna exhibits a peak gain of 9.24 dB, and the radiation efficiency of the MIMO antenna is 78.6% as shown in Figure 18, for the entire range of frequencies.

5. COMPARATIVE STUDY

Table 2 presents a comparative study of the proposed MIMO antenna with the other antennas reported in the literature. It can be observed from the table that the proposed MIMO antenna has various advantages over the MIMO antennas presented in literature [23–31], such as antenna size, number of radiating elements, gain, impedance bandwidth, efficiency, and isolation among MIMO antenna elements. In addition, a defective ground plane structure is used for the proposed quad element MIMO antenna to ensure a stable operation, along with the four radiating elements arranged in anti-parallel mode and orthogonal to each other.

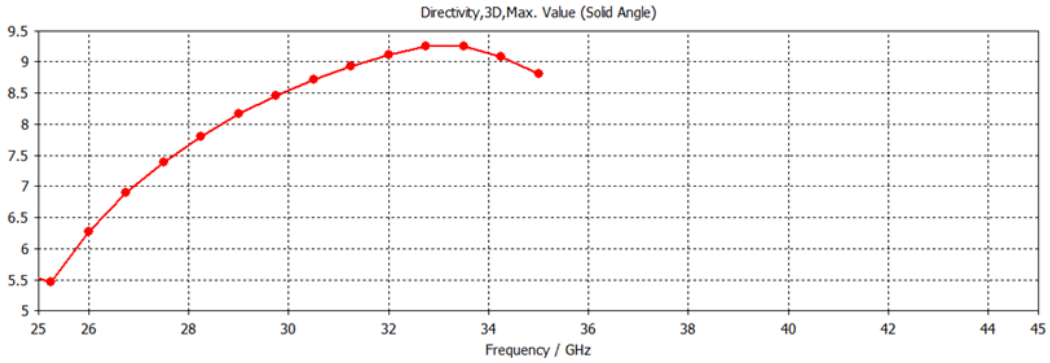

Figure 17. Plot of Maximum gain over frequency of the MIMO antenna.

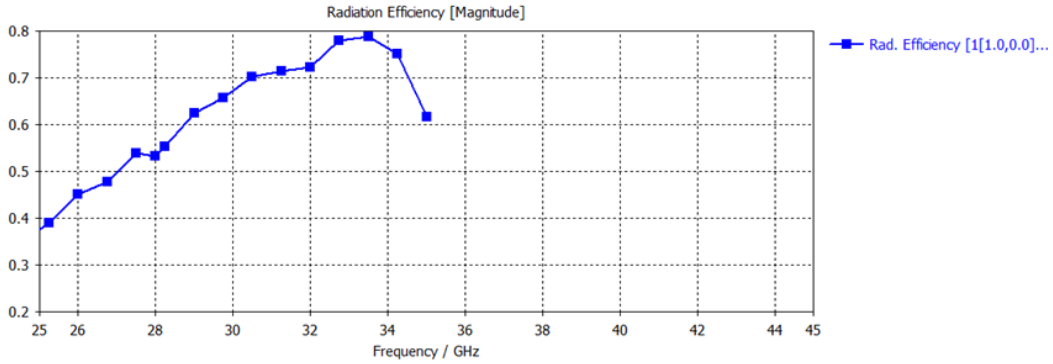

Figure 18. Plot of Radiation Efficiency over frequency of the MIMO antenna.

Table 2. A comparative study of the proposed MIMO antenna with other antennas.

Reference Paper	No. of ports	Size (mm^3)	Approximate Return Loss (dB)	Isolation (dB)	Bandwidth	Peak Gain (dB)	Total Eff. (%)	ECC
[23]	4	$30 \times 35 \times 0.76$	-35	> 10	25.5–29.6	8.3	80–85	< 0.01
[24]	8	$145 \times 75 \times 6$	-10	> 15	25.5–29.6	1.6–4.5	42–73	< 0.16
[25]	4	$90 \times 90 \times 1.6$	-50	> 13	3–9	11–12	-	-
[26]	8	$150 \times 75 \times 7$	-25	> 11.5	3.4–3.6, 4.8–5.1	-	48–85	< 0.16
[27]	-	-	-30	$> -$	21–34	9	-	-
[28]	4	$19 \times 19 \times 7.608$	-40	> 20	26–29.5	14	-	< 0.015
[29]	-	$30 \times 30.5 \times 0.508$	-30	$> -$	24–28	7.4	-	-
[30]	2	$66.8 \times 40 \times 0.8$	-30	> 15	2.6–13	0.76–6.02	> 75	< 0.02
[31]	4	$158 \times 77.8 \times 0.38$	-35	> 17	24–28	0.76–6.02	< 75	< 0.001
[32]	4	$80 \times 80 \times 1.57$	-35	> 20	23–40	12	< 75	< 0.0014
Proposed Design	4	$20 \times 20 \times 0.8$	-35	> 18	27.5–40	9.24	> 77	< 0.0013

6. CONCLUSIONS

In this paper, a four element MIMO antenna working at centre frequency of 28 GHz with a proper impedance matching is designed, simulated, and tested on an RT Duroid 5880 substrate for 5G applications. The proposed MIMO antenna design is very simple in structure, very compact in size with the dimensions of $20 \times 20 \times 0.8\,\text{mm}^3$ and has peak gain 9.24 dB and bandwidth 2.1 GHz. The simulated and measured results demonstrate that the proposed MIMO antenna has better performance than the antennas listed in the Table 2, in terms of reflection coefficient, mutual coupling, radiation pattern characteristics, gain, bandwidth, efficiency, and correlation coefficient.

REFERENCES

1. Zhang, J., X. Yu, and K. B. Letaief, "Hybrid beam forming for 5G and beyond millimeter-wave systems: A holistic view," *IEEE Open Journal of the Communications Society*, Vol. 1, 77–91, 2019.
2. Przesmycki, R., M. Bugaj, and L. Nowosielski, "Broadband microstrip antenna for 5G wireless systems operating at 28 GHz," *Electronics*, Vol. 10, 1, 2021.
3. Kim, G. and S. Kim, "Design and analysis of dual polarized broadband microstrip patch antenna for 5G mmwave antenna module on FR4 substrate," *IEEE Access*, Vol. 9, 64306–64316, 2021.
4. Almashhdany, M. B., A. A. Oras, M. S. Ahmed, A. Mohamed, H. Naba, and A. Fatima, "Design of multi-band slotted mmwave antenna for 5G mobile applications," *Proceedings of the IOP Conference Series: Materials Science and Engineering*, Vol. 881, No. 1, 012150, April 2020.
5. Haroon, M. S., F. Muhammad, G. Abbas, Z. H. Abbas, A. Kamal, M. Waqas, and S. Kim, "Interference management in ultra-dense 5G networks with excessive drone usage," *IEEE Access*, 1–10, 2020.
6. Khan, J., D. A. Sehrai, and U. Ali, "Design of dual band 5G antenna array with SAR analysis for future mobile handsets," *J. Electr. Eng. Technol.*, Vol. 14, 809–816, 2019.
7. Pervez, M. M., Z. H. Abbas, F. Muhammad, and L. Jiao, "Location-based coverage and capacity analysis of a two tier HetNet," *IET Commun.*, Vol. 11, 1067–1073, 2017.
8. Sun, L., Y. Li, Z. Zhang, and Z. Feng, "Wideband 5G MIMO antenna with integrated orthogonal-mode dual-antenna pairs for metal-rimmed smartphones," *IEEE Trans. Antennas Propag.*, Vol. 68, 2494–2503, 2020.
9. Abdullah, M., S. H. Kiani, and A. Iqbal, "Eight element multiple-input multiple-output (MIMO) antenna for 5G mobile applications," *IEEE Access*, Vol. 7, 134488–134495, 2019.
10. Yuan, X., W. He, K. Hong, C. Han, Z. Chen, and T. Yuan, "Ultra-wideband MIMO antenna system with high element-isolation for 5G smartphone application," *IEEE Access*, Vol. 8, 56281–56289, 2020.
11. Altaf, A., M. A. Alsunaidi, and E. Arvas, "A novel EBG structure to improve isolation in MIMO antenna," *Proceedings of the IEEE USNC-URSI Radio Science Meeting (Joint with AP-S Symposium)*, 105–106, San Diego, CA, USA, July 9–14, 2017.
12. Wang, F., Z. Duan, X. Wang, Q. Zhou, and Y. Gong, "High isolation millimeter-wave wideband MIMO antenna for 5G communication," *Int. J. Antennas Propag.*, 4283010, 2019.
13. Abdullah, M., S. H. Kiani, L. F. Abdulrazak, A. Iqbal, M. A. Bashir, S. Khan, and S. Kim, "High-performance multiple-input multiple-output antenna system for 5G mobile terminals," *Electronics*, Vol. 8, 1090, 2019.
14. Haroon, M. S., Z. H Abbas, G. Abbas, and F. Muhammad, "SIR analysis for non-uniform HetNets with Joint decoupled association and interference management," *Comput. Commun.*, Vol. 155, 48–57, 2020.
15. Haroon, M. S., Z. H. Abbas, F. Muhammad, and G. Abbas, "Coverage analysis of cell edge users in heterogeneous wireless networks using Stienen's model and RFA scheme," *Int. J. Commun. Syst.*, Vol. 33, e4147, 2019.
16. Khan, J., D. A. Sehrai, M. A. Khan, H. A. Khan, S. Ahmad, A. Ali, A. Arif, A. A. Memon, and S. Khan, "Design and performance comparison of rotated Y-shaped antenna using different metamaterial surfaces for 5G mobile devices," *Comput. Mater. Contin.*, Vol. 60, 409–420, 2019.

17. Wang, P., Y. Li, L. Song, and B. Vucetic, "Multi-gigabit millimeter waves wireless communications for 5G: From fixed access to cellular networks," *IEEE Commun. Mag.*, Vol. 53, 168–178, 2015.
18. Sulyman, A. I., A. Alwarafy, G. R. MacCartney, T. S. Rappaport, and A. Alsanie, "Directional radio propagation path loss models for millimeter-wave wireless networks in the 28-, 60-, and 73-GHz bands," *IEEE Trans. Wirel. Commun.*, Vol. 15, 6939–6947, 2016.
19. Shayea, I., T. A. Rahman, M. H. Azmi, and M. R. Islam, "Real measurement study for rain rate and rain attenuation conducted over 26 GHz microwave 5G link system in Malaysia," *IEEE Access*, Vol. 6, 19044–19064, 2018.
20. Zhang, J., X. Ge, Q. Li, M. Guizani, and Y. Zhang, "5G millimeter-wave antenna array: Design and challenges," *IEEE Wirel. Commun.*, Vol. 24, 106–112, 2017.
21. Roh, W., J. Y. Seol, J. Park, B. Lee, J. Lee, Y. Kim, J. Cho, K. Cheun, and F. Aryanfar, "Millimeter-wave beamforming as an enabling technology for 5G cellular communications: Theoretical feasibility and prototype results," *IEEE Commun. Mag.*, Vol. 52, 106–113, 2014.
22. Khalily, M., R. Tafazolli, P. Xiao, and A. A. Kishk, "Broadband mm-wave microstrip array antenna with improved radiation characteristics for different 5G applications," *IEEE Trans. Antennas Propag.*, Vol. 66, 4641–4647, 2018.
23. Khalid, M., S. Iffat Naqvi, N. Hussain, M. Rahman, S. S. Mirjavadi, M. J. Khan, and Y. Amin, "4 port MIMO antenna with defected ground structure for 5G millimeter wave applications," *Electronics*, Vol. 9, 71, 2020.
24. Liu, Y., A. Ren, H. Liu, H. Wang, and C. Sim, "Eight-port MIMO array using characteristic mode theory for 5G smartphone applications," *IEEE Access*, Vol. 7, 45679–45692, 2019.
25. Haq, M. A. U., M. A. Khan, and M. R. Islam, "MIMO antenna design for future 5G wireless communication systems," *Software Engineering, Artificial Intelligence, Networking and Parallel/Distributed Computing*, 653, Springer, Cham, Switzerland, 2016.
26. Guo, J., L. Cui, C. Li, and B. Sun, "Side-edge frame printed eight-port dual-band antenna array for 5G smartphone applications," *IEEE Trans. Antennas Propag.*, Vol. 66, 7412–7417, 2018.
27. Yang, B., Z. Yu, Y. Dong, J. Zhou, and W. Hong, "Compact tapered slot antenna array for 5G millimeter-wave massive MIMO systems," *IEEE Trans. Antennas Propag.*, Vol. 65, 6721–6727, 2017.
28. Hussain, N., M. Jeong, J. Park, and N. Kim, "A broadband circularly polarized fabry-perot resonant antenna using a single-layered PRS for 5G MIMO applications," *IEEE Access*, Vol. 7, 42897–42907, 2019.
29. Jiang, H., L. Si, W. Hu, and X. Lv, "A symmetrical dual-beam bowtie antenna with gain enhancement using metamaterial for 5G MIMO applications," *IEEE Photonics J.*, Vol. 11, 1–9, 2019.
30. Patre, S. R. and S. P. Singh, "Broadband multiple-input–multiple-output antenna using castor leaf-shaped quasi-self-complementary elements," *IET Microwaves, Antennas & Propagation*, Vol. 10, 1673–1681, IET, Hertford, UK, 2016.
31. Abbas, E. A., M. Ikram, A. T. Mobashsher, and A. Abbosh, "MIMO antenna system for multi-band millimeter-wave 5G and wideband 4G mobile communications," *IEEE Access*, Vol. 7, 181916–181923, 2019.
32. Sehrai, D. A., M. Abdullah, A. Altaf, S. H. Kiani, F. Muhammad, M. Tufail, M. Irfan, A. Glowacz, and S. Rahman, "A novel high gain wideband MIMO antenna for 5G millimeter wave applications," *Electronics*, Vol. 9, 1031, 2020.
33. Morabito, A. F., A. R. Laganà, and T. Isernia, "Optimizing power transmission in given target areas in the presence of protection requirements," *IEEE Antennas and Wireless Propagation Letters*, Vol. 14, 44–47, 2015.